Maximum Nuclear-Recoil Energy in Elastic Dark Matter–Nucleus Scattering

Belkacem E. Khodja

Boston University, 700 Commonwealth Avenue, Boston, Massachusetts 02215, USA

khodja@bu.edu

Abstract. Multiple independent observations indicate that most of the matter in the universe is nonluminous and nonbaryonic. A leading experimental strategy is direct detection, in which a dark matter particle scatters elastically from a target nucleus, producing a nuclear recoil. In this paper, we derive the kinematic maximum recoil energy expected from elastic scattering as a function of the dark matter mass, the target-nucleus mass, and the incident speed (taking a representative galactic speed $v \sim 10^{-3}c$). Using representative target materials found in current experiments (cryogenic crystals, scintillators, and liquid noble gases), we evaluate how the maximum recoil energy scales across the low-mass and high-mass regimes. The results show a rapid rise in recoil energy when the dark matter mass is below the target-nucleus mass, followed by saturation in the heavy dark matter limit; for ($v \sim 10^{-3}c$), the saturation values are ~ 245 keV for xenon and ~ 52.3 keV for silicon. This simple kinematic analysis helps clarify how target choice constrains energy thresholds and, as a result, influences experimental sensitivity to different dark matter mass ranges without computing event rates or experimental limits.

INTRODUCTION

Understanding the composition of the universe remains a central goal of modern physics. Astronomical measurements consistently imply that the mass inferred from gravity is much larger than the mass that can be accounted for by luminous stars, gas, and dust [1–3]. Early evidence came from Zwicky's analysis of galaxy clusters, where velocity dispersions suggested a large "missing mass," and later from Rubin and Ford's analysis of galaxy rotation curves as well as studies on gravitational lensing and precision cosmology [1–5]. Collectively, these observations motivate the hypothesis of dark matter: a stable, nonluminous component that interacts predominantly through gravity and constitutes most of the matter content of the universe [1–3]. Establishing the particle nature of dark matter is therefore a major experimental objective [1–3,6].

Following the original dynamical anomalies reported in clusters and galaxies, the field has developed several complementary search strategies [1–3]. Indirect-detection experiments look for dark matter annihilation or decay products (such as gamma rays, antimatter, or neutrinos), while collider searches attempt to produce dark matter in high-energy particle collisions and infer its presence through missing momentum [2,3,6]. Direct-detection experiments, the focus here, aim to observe the tiny energy deposition from a dark matter particle scattering inside a terrestrial detector [6–8]. Because each approach probes different interaction models and systematics, consistency across multiple techniques will be essential for a convincing discovery [2,3,6].

Direct-detection methods aim to observe dark matter through its interaction with ordinary matter, most commonly via elastic scattering from nuclei [6-9]. In a typical event, a dark matter particle transfers a small fraction of its kinetic energy to a target nucleus, generating a recoil that can be measured through scintillation light, ionization charge, phonons, or a combination of channels, depending on the detector technology [6–9]. The measurable recoil spectrum depends on both particle physics (interaction type and mass) and astrophysics (the local dark matter velocity distribution) [6–8,10]. A useful, detector-independent quantity is the maximum recoil energy permitted by kinematics. In the following, we derive the maximum possible nuclear-recoil energy and use it to interpret how detector thresholds and target masses jointly shape sensitivity across candidate dark matter masses [6,7,12]. This sets the upper edge of the recoil range and provides intuition for which target materials are best matched to a given dark matter mass scale [7,8,12].

RECOIL-ENERGY KINEMATICS

In the case of direct detection, we consider elastic scattering of a dark matter particle of mass m_χ from a target nucleus of mass M_T, as shown in Fig. 1. As described in [12], for non-relativistic scattering, the nuclear-recoil energy E_R is related to the momentum transfer magnitude $q = \|\mathbf{q}\|$ through

$$q = (2\, M_T\, E_R)^{\frac{1}{2}}. \tag{1}$$

Writing q in terms of the reduced mass $\mu = m_\chi M_T/(m_\chi + M_T)$, the incident relative speed v, and the center-of-mass (CM) frame angle θ between the incoming and outgoing relative momenta, one obtains

$$q = \, 2\mu v \sin\frac{\theta}{2}. \tag{2}$$

Equating the right-hand sides of Eqs. (1) and (2) and then solving for E_R, one obtains

$$E_R = \frac{2\mu^2 v^2}{M_T}\, \sin^2\frac{\theta}{2}. \tag{3}$$

To maximize E_R for backward scattering, set $\theta = \pi$. Hence, the maximum recoil energy $E_{R,max}$ is

$$E_{R,max} = \frac{2\mu^2 v^2}{M_T}. \tag{4}$$

This maximum recoil energy is the key quantity used in the calculations and comparisons that follow.

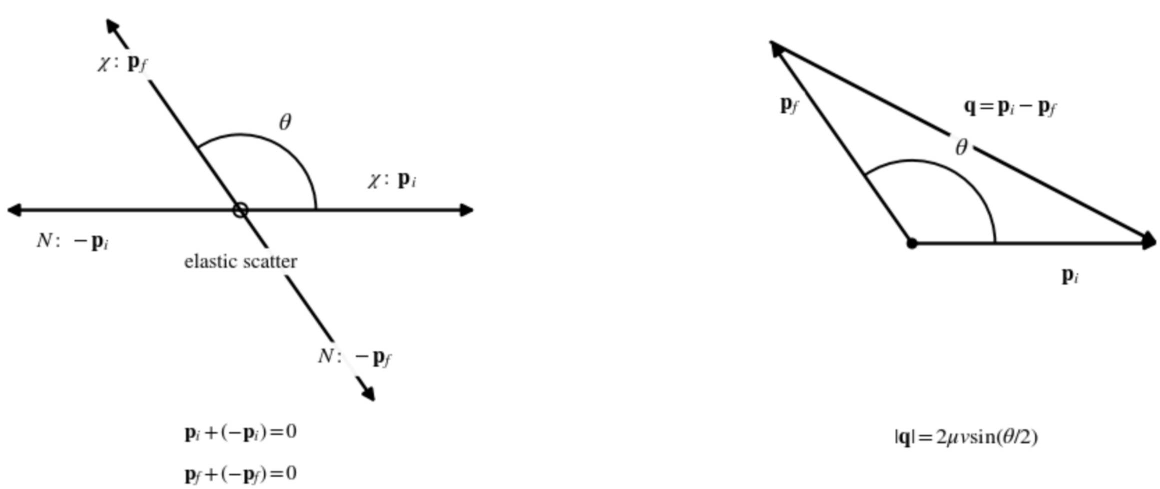

(a) (b)

FIGURE 1. (a) Schematic of elastic scattering in the center-of-mass (CM) frame. The target nucleus is labeled *N* and the dark matter particle is labeled χ. The total momentum of *N* and χ before and after the scattering is 0. Furthermore, the momentum of *N* is equal in magnitude but opposite in direction to χ before and after the scattering. (b) Momentum-transfer geometry in the CM frame. The CM frame angle θ between the incoming and outgoing relative momenta is shown alongside the momentum transfer. By setting $\theta = \pi$, we obtain backscattering.

NUMERICAL RESULTS

We plot Eq. (4) as a function of the dark matter mass m_x for several target materials used in direct-detection technologies: xenon in liquid noble gas chambers, silicon in cryogenic crystals, and sodium and iodine in scintillating crystals. We set $c = 1$ and M_T as provided in Table 1 in Appendix A. We also set $v \sim 10^{-3}c$ as a representative galactic dark matter speed. This value is not intended to model the full local velocity distribution; rather, it provides a simple benchmark of the same order as the velocity that is commonly used, which is $v \sim 220$ km/s [11].

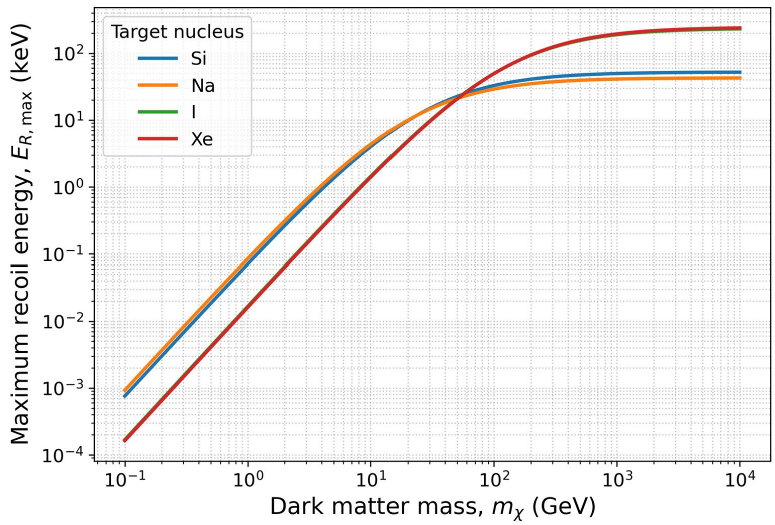

FIGURE 2. Plot of maximum recoil energy $E_{R,max}$ against the dark matter mass m_x for the target materials in Table 1.

The dark matter mass range is chosen to span a broad range, from sub-GeV-scale candidates to multi-TeV weakly interacting massive particle (WIMP)-scale candidates. It is not meant to include ultralight candidates such as axions. The elastic, nonrelativistic treatment used here is appropriate as a first-pass kinematic model for the mass ranges we consider as well as our choice of the galactic dark matter speed. From Fig. 2 we observe that the maximum recoil energy from elastic scattering plateaus for all target materials. This follows because in the large dark matter mass limit ($m_\chi \gg M_T$), the reduced mass μ approaches the target mass M_T, so the kinematic maximum recoil energy becomes approximately target dependent and independent of m_χ. In this limit, the plateau values are $E_{R,max} \sim 52.3, 42.8, 236,$ and 245 keV for silicon, sodium, iodine, and xenon, respectively. For an experiment to be sensitive to such recoils, the detector's effective threshold must lie below the relevant recoil energies; at the kinematic level this can be expressed as

$$E_{R,max} \geq E_T. \quad (5)$$

However, E_T is experiment dependent because detectors measure observable quantities such as ionization and scintillation light rather than measuring the true nuclear-recoil energy E_R directly. Calibration is then used to convert these observables into recoil-energy estimates. Thresholds are often quoted either in keVnr (nuclear-recoil energy) or in keVee (electron-equivalent energy), and converting between them requires a detector-response model and calibration.

For example, in scintillating crystals composed of sodium iodide, the experimental threshold is often quoted in electron-equivalent energy, and nuclear recoils appear at reduced visible energies due to quenching. This makes the mapping between a detector's quoted threshold and the underlying nuclear-recoil energy nontrivial, and it reinforces why kinematic limits alone are not sufficient to claim sensitivity without a detector-response model. This point is especially relevant for canonical WIMP searches, where nuclear recoils are the primary signal channel. The trend in Fig. 2 illustrates an important design principle: at fixed incident speed, heavier targets tend to produce larger maximum recoil energies for a given dark matter mass, while lighter targets can provide improved kinematic matching to low-mass dark matter. In the heavy dark matter limit ($m_\chi \gg M_T$), $E_{R,max}$ approaches a target-dependent constant proportional to $M_T v^2$, whereas in the light dark matter regime ($m_\chi \ll M_T$), the maximum recoil energy falls rapidly with m_χ. Explicitly, the reduced mass becomes $\mu \sim m_\chi$, so Eq. (4) becomes $E_{R,max} \sim 2{m_\chi}^2 v^2/M_T$. Hence, the maximum recoil energy scales quadratically with dark matter mass: decreasing m_χ by a factor of 10 decreases $E_{R,max}$ by a factor of 100.

These scaling behaviors help explain why modern experimental programs deploy multiple target materials to cover a broad dark matter mass range, particularly across the WIMP-motivated mass scales. Scintillating detectors such as COSINE-100 use sodium and iodine targets to search for WIMPs [13]. On the other hand, cryogenic experiments such as SuperCDMS use silicon crystals to explore smaller dark matter masses within the sub-GeV range [14]. Liquid Xenon detectors such as LUX and XENON1T measure scintillation and ionization in dual-phase time-projection chambers in their search for WIMPs [15,16].

CONCLUSION

We used elastic-scattering kinematics to derive and visualize the maximum nuclear-recoil energy expected in direct-detection experiments as a function of dark matter mass and target nucleus mass. By comparing representative detector materials, we highlighted the transition from the low-mass regime, where recoil energies are strongly suppressed, to the high-mass regime, where the maximum recoil energy saturates. Although a full sensitivity projection requires detector-specific efficiencies, backgrounds, and response models, the maximum-recoil framework provides a clear first-pass guide for interpreting energy thresholds and for understanding why a portfolio of target materials is valuable. Continued improvements in low-threshold technologies, background rejection, and exposure will be critical for advancing discovery potential across the remaining viable dark matter parameter space.

ACKNOWLEDGEMENTS

We thank Prof. Zeynep Demiragli for her advice and help.

REFERENCES

1. G. Bertone and D. Hooper, "A history of dark matter," Rev. Mod. Phys. **90**, 045002 (2018).
2. L. Bergström, "Dark matter evidence, particle physics candidates and detection methods," Ann. Phys. (Berlin) **524**, 479–496 (2012).
3. S. Navas, C. Amsler, T. Gutsche, C. Hanhart, J. J. Hernández-Rey, C. Lourenço, A. Masoni, M. Mikhasenko, R. E. Mitchell, C. Patrignani, et al., "Review of particle physics–dark matter," Phys. Rev. D **110**, 030001 (2024).
4. F. Zwicky, "Die Rotverschiebung von extragalaktischen Nebeln," Helv. Phys. Acta **6**, 110–127 (1933).
5. V. C. Rubin and W. K. Ford, Jr., "Rotation of the Andromeda Nebula from a spectroscopic survey of emission regions," Astrophys. J. **159**, 379–403 (1970).
6. J. Billard, E. Figueroa-Feliciano, and L. Strigari, "Direct detection of dark matter—APPEC committee report," Rep. Prog. Phys. **85**, 056201 (2022).
7. M. Schumann, "Direct detection of WIMP dark matter: Concepts and status," J. Phys. G **46**, 103003 (2019).
8. T. M. Undagoitia and L. Rauch, "Dark matter direct-detection experiments," J. Phys. G **43**, 013001 (2016).
9. L. Baudis, "Dark matter direct detection: status, results and future plans," J. Phys.: Conf. Ser. 3162 012007, 2025.
10. K. Freese, M. Lisanti, and C. Savage, "Colloquium: Annual modulation of dark matter," Rev. Mod. Phys. **85**, 1561 (2013).
11. N. W. Evans, C. A. J. O'Hare, and C. McCabe, "Refinement of the standard halo model for dark matter searches in light of the Gaia Sausage," Phys. Rev. D **99**, 023012 (2019).
12. J. D. Lewin and P. F. Smith, "Review of mathematics, numerical factors, and corrections for dark matter experiments based on elastic nuclear recoil," Astropart. Phys. **6**, 87–112 (1996).
13. G. Adhikari, P. Adhikari, E. Barbosa de Souza, N. Carlin, S. Choi, M. Djamal, A. C. Ezeribe, C. Ha, I. S. Hahn, E. J. Jeon, et al., "Search for a dark matter-induced annual modulation signal in NaI(Tl) with the COSINE-100 experiment," Phys. Rev. Lett. **123**, 031302 (2019).
14. R. Agnese, A. J. Anderson, T. Aramaki, I. Arnquist, W. Baker, D. Barker, R. Basu Thakur, D. A. Bauer, M. A. Bowles, P. L. Bring, et al., "Projected sensitivity of the SuperCDMS SNOLAB experiment," Phys. Rev. D **95**, 082002 (2017).
15. D. S. Akerib, H. M. Araújo, X. Bai, A. J. Bailey, J. Balajthy, S. Bedikian, E. Bernard, A. Bernstein, A. Bolozdynyaet, A. Bradley, D. Bryam, et al., "First results from the LUX dark matter experiment at the Sanford Underground Research Facility," Phys. Rev. Lett. **112**, 091303 (2014).
16. E. Aprile, J. Aalbers, F. Agostini, M. Alfonsi, L. Althueser, F. D. Amaro, M. Anthony, F. Arneodo, L. Baudis, B. Bauermeister, et al., "Dark matter search results from a one ton-year exposure of XENON1T," Phys. Rev. Lett. **121**, 111302 (2018).

APPENDIX A

TABLE 1. Nuclear target masses used for the recoil-energy calculations (representative materials used in elastic-scattering direct-detection experiments) [5].

Target Material	M_T (GeV)
Silicon (Si)	28.1
Sodium (Na)	23
Iodine (I)	127
Xenon (Xe)	131